Sleep Architecture in Mice Is Shaped by the Transcription Factor AP-2β

Ayaka Nakai,*,† Tomoyuki Fujiyama,* Nanae Nagata,* Mitsuaki Kashiwagi,* Aya Ikkyu,* Marina Takagi,* Chika Tatsuzawa,* Kaeko Tanaka,* Miyo Kakizaki,* Mika Kanuka,* Taizo Kawano,* Seiya Mizuno,‡ Fumihiro Sugiyama,‡ Satoru Takahashi,‡ Hiromasa Funato,*,§ Takeshi Sakurai,*,,†† Masashi Yanagisawa,*,††,‡‡,§§ and Yu Hayashi*,***,1**

*International Institute for Integrative Sleep Medicine (WPI-IIIS), †PhD Program in Neuroscience, Comprehensive Human Sciences, Graduate School of Comprehensive Human Sciences, ‡Laboratory Animal Resource Center, **Faculty of Medicine, ††Life Science Center for Survival Dynamics, Tsukuba Advanced Research Alliance (TARA), and §§R&D Center for Frontiers of MIRAI in Policy and Technology, University of Tsukuba, 305-8575, Japan, §Department of Anatomy, Faculty of Medicine, Toho University, Tokyo 143-8540, Japan, ‡‡Department of Molecular Genetics, University of Texas Southwestern Medical Center, Dallas, Texas 75390, and ***Department of Human Health Sciences, Graduate School of Medicine, Kyoto University, 606-8507, Japan

ORCID IDs: 0000-0001-6420-2283 (T.F.); 0000-0002-2787-9700 (H.F.); 0000-0003-4474-6253 (T.S.); 0000-0002-7358-4022 (M.Y.); 0000-0001-5007-4532 (Y.H.)

ABSTRACT The molecular mechanism regulating sleep largely remains to be elucidated. In humans, families that carry mutations in *TFAP2B*, which encodes the transcription factor AP-2β, self-reported sleep abnormalities such as short-sleep and parasomnia. Notably, AP-2 transcription factors play essential roles in sleep regulation in the nematode *Caenorhabditis elegans* and the fruit fly *Drosophila melanogaster*. Thus, AP-2 transcription factors might have a conserved role in sleep regulation across the animal phyla. However, direct evidence supporting the involvement of TFAP2B in mammalian sleep was lacking. In this study, by using the CRISPR/Cas9 technology, we generated two *Tfap2b* mutant mouse strains, $Tfap2b^{K144}$ and $Tfap2b^{K145}$, each harboring a single-nucleotide mutation within the introns of *Tfap2b* mimicking the mutations in two human kindreds that self-reported sleep abnormalities. The effects of these mutations were compared with those of a *Tfap2b* knockout allele ($Tfap2b^{-}$). The protein expression level of TFAP2B in the embryonic brain was reduced to about half in $Tfap2b^{+/-}$ mice and was further reduced in $Tfap2b^{-/-}$ mice. By contrast, the protein expression level was normal in $Tfap2b^{K145/+}$ mice but was reduced in $Tfap2b^{K145/K145}$ mice to a similar extent as $Tfap2b^{-/-}$ mice. $Tfap2b^{K144/+}$ and $Tfap2b^{K144/K144}$ showed normal protein expression levels. $Tfap2b^{+/-}$ female mice showed increased wakefulness time and decreased nonrapid eye movement sleep (NREMS) time. By contrast, $Tfap2b^{K145/+}$ female mice showed an apparently normal amount of sleep but instead exhibited fragmented NREMS, whereas $Tfap2b^{K144/+}$ male mice showed reduced NREMS time specifically in the dark phase. Finally, in the adult brain, *Tfap2b-LacZ* expression was detected in the superior colliculus, locus coeruleus, cerebellum, and the nucleus of solitary tract. These findings provide direct evidence that TFAP2B influences NREMS amounts in mice and also show that different mutations in *Tfap2b* can lead to diverse effects on sleep architecture.

KEYWORDS Char syndrome; mouse; sleep; transcription factor

SLEEP is a physiological state widely observed in animals. However, the molecular pathways involved in regulating sleep, and to what the extent they are conserved among vertebrates and invertebrates, remain largely unknown. In humans, natural short sleepers exhibit a reduced amount of time in sleep without reporting daytime fatigue [reviewed in Shi *et al.* (2017)]. In cases where the natural short sleep trait is hereditary, it is expected that the identification of the causal gene might lead to the understanding of the molecules that control sleepiness. In addition, recent studies using invertebrate animal models suggest that sleep-regulatory mechanisms are at least partly conserved at the molecular level between vertebrates and invertebrates [reviewed in (Miyazaki

doi: https://doi.org/10.1534/genetics.120.303435
Manuscript received June 13, 2020; accepted for publication August 31, 2020; published Early Online September 2, 2020.
Supplemental material available at figshare: https://doi.org/10.25386/genetics.12904568.
[1]Corresponding author: Kyoto University, 53 Kawahara-cho, Shogoin, Sakyo-ku, Kyoto 606-8507, Japan. E-mail: hayashi.yu.fp@u.tsukuba.ac.jp

et al. 2017)]. For example, a gain-of-function mutation in the salt-inducible kinase three leads to a drastic increase in the amount of nonrapid eye movement sleep (NREMS) in mice, whereas its ortholog in the nematode *Caenorhabditis elegans* promotes developmentally timed sleep and the ortholog in the fruit fly *Drosophila melanogaster* promotes total sleep (Funato *et al.* 2016). Thus, studies using invertebrate animal models are also expected to lead to the identification of key molecules that contribute to sleep regulation across animal phyla.

In this study, we focused on the transcription factor AP-2β (TFAP2B). TFAP2B is a member of the AP-2 transcription factor family, which is involved in diverse processes including cell proliferation, differentiation, and apoptosis at both developmental and mature stages [reviewed in Eckert *et al.* (2005)]. In mice, *Tfap2b* knockout pups die shortly after birth due to renal failure (Moser *et al.* 1997, 2003). *Tfap2b* is also crucial for limb formation and differentiation of several neuronal cells (Seok *et al.* 2008; Jin *et al.* 2015; Seki *et al.* 2015). In humans, mutations in *TFAP2B* lead to Char syndrome (MIM 169100) (Satoda *et al.* 2000). Char syndrome is a congenital disease characterized by patent ductus arteriosus, facial dysmorphism, and hand anomalies (Davidson 1993). Notably, two human kindreds with Char syndrome, kindred 144 and 145, self-reported abnormalities in sleep, namely parasomnia (sleep-walking) and short-sleep, respectively (Mani *et al.* 2005). The two kindreds harbor a mutation in the introns of *TFAP2B*, thus implying the involvement of TFAP2B in sleep regulation.

Moreover, in the nematode *Caenorhabditis elegans*, the ortholog APTF-1 is crucial for specification of the sleep-promoting neuron RIS, and *aptf-1* mutants exhibit severely reduced quiescence during both developmentally timed sleep and stress-induced sleep (Turek *et al.* 2013, 2016; Konietzka *et al.* 2020). In addition, in the fruit fly *Drosophila melanogaster*, knockdown of neuronal TFAP-2 results in reduced night-time sleep (Kucherenko *et al.* 2016). These findings, in combination with recent studies supporting that the molecular mechanisms of sleep are conserved between mammals and invertebrates, suggest that mammalian TFAP2B is involved in sleep regulation. However, in case of mammals, conclusive evidence was lacking because the direct effect of mutating this gene was unknown. In this study, we tested whether sleep is affected in mice deficient for *Tfap2b*. Furthermore, considering that the human kindreds 144 and 145 self-reported totally different sleep abnormalities, we generated two mutant mouse strains, each carrying a mutation in *Tfap2b* that mimicked the mutation in the human kindreds 144 and 145 by utilizing CRISPR/Cas9 genome editing, and examined their effects on sleep architecture.

Methods

Animals

All animal experiments were approved by the institutional animal care and use committee of the University of Tsukuba. All animals were maintained according to the institutional guidelines of the animal facilities of the Laboratory of Animal Resource Center, University of Tsukuba. Mice were maintained and bred in International Institute for Integrative Sleep Medicine under 12-hr light/dark cycle and free access to food and water. Male and female mice of 10–13 weeks of age were used for sleep analyses.

To obtain *Tfap2b*$^{+/-}$ mice, *Tfap2b*$^{tm1a(EUCOMM)Wtsi/+}$ mice from KOMP (Knockout Mouse Project) (Skarnes *et al.* 2011) were crossed with mice carrying the *Ayu1*-cre allele (Niwa *et al.* 1993) to remove a genomic DNA fragment containing *Tfap2b* exon3 and a neomycin resistant cassette flanked by loxP. The *Tfap2b*$^{tm1a(EUCOMM)Wtsi}$ allele contains an IRES:lacZ trapping cassette with *Engrailed* (En2) splice acceptor sequences immediately after *Tfap2b* exon2 and is followed by a poly-A transcription termination signals. F1 offspring were then maintained by crossing with C57BL/6J mice.

Generation of Tfap2b^{K144} and Tfap2b^{K145} mice by CRISPR/Cas9 technology

The *Tfap2b*^{K144} point mutation (c.601+5G > A) and the *Tfap2b*^{K145} point mutation (c.822-1G > C) were introduced to the mouse genome by CRISPR/Cas9 technology as previously reported with some modifications (Sato *et al.* 2018). The guide RNA (gRNA) was synthesized and purified using the GeneArt Precision gRNA Synthesis Kit (ThermoFisher). The sequences of the gRNA were 5′-GTCAGTCATTAAAAAAGGTA-3′ for *Tfap2b*^{K144} and 5′-TTTTCGATTTGGCTCTGCAG-3′ for *Tfap2b*^{K145}. The donor oligonucleotides for *Tfap2b*^{K144} and *Tfap2b*^{K145} were both 101 bases (Integrated DNA Technologies), in which the desired point mutations were introduced. Pregnant mare serum gonadotropin and human chorionic gonadotropin were injected intraperitoneally into female C57BL/6J mice (Charles River Laboratories), and unfertilized oocytes were collected from their oviducts. We then performed *in vitro* fertilization with these oocytes and sperm from male C57BL/6J mice. The gRNA, donor oligonucleotide, and GeneArt Platinum Cas9 Nuclease (ThermoFisher) were electroporated into zygotes using a NEPA 21 electroporator (NEPAGNENE). After electroporation, embryos developed to the two-cell stage in KSOM-AA medium. The next day, the electroporated two-cell embryos were transferred into pseudopregnant ICR mice. We amplified the genomic region including the target sites and PAM sequence by PCR with the following primers, and confirmed the insertion of the desired mutation and the absence of additional mutations. *Tfap2b*^{K144}: 5′-AAAACCTC CATTTGTGGGTTAAT-3′ and 5′-TGCCAGTGTTGCTCTGAT CT-3′; *Tfap2b*^{K145}: 5′- TCTGGATCCACTGCCCTAAC-3′ and 5′- CACTCATAAGGGCACAGCAA-3′. F0 mice were mated with WT C57BL/6J mice for at least four generations before sleep recording.

Genotyping

Genotyping of *Tfap2b*$^{+/-}$ mice was performed using the following primers: 5′-GACATCCTACAATGCACAGCT-3′, 5′-CAA CGGGTTCTTCTGTTAGTCC-3′, and 5′-TTGCTGTGAGCTAA

GAGCTTC-3′ (WT: 381 bp, *Tfap2b*$^{-}$ mutant: 529 bp). For routine genotyping of *Tfap2b*^{K145} and *Tfap2b*^{K144}, we applied the dCAPS method using the following combinations of primer pairs and restriction enzymes.

Tfap2b^{K144}: 5′-AAAACCTCCATTTGTGGGTTAAT-3′ and 5′-AGACATTGAAATCTTTGCTTACTTTTGGAAGAAAGGATC-3′ followed by digestion by *Bam*HI to specifically digest the WT allele (WT: 183 bp, *Tfap2b*^{K144} mutant: 223 bp).

Tfap2b^{K145}: 5′-GAATGTTAATTCTCACCAGTGCA-3′ and 5′-CACTCATAAGGGCACAGCAA-3′ followed by digestion by *Apa*LI to specifically digest the mutant allele (WT: 266 bp, *Tfap2b*^{K145} mutant: 247 bp).

Reverse transcription-PCR

Brains of mouse embryos were harvested 18 days after detection of vaginal plugs (embryonic period 18.5; E18.5). Each brain was divided in half at the midline and frozen with liquid nitrogen. Samples of brains mixed sex were used. Total RNA was extracted from the samples using TRIzol reagent (ThermoFisher). Genomic DNA was digested and reverse transcription (RT) was performed with oligo-dT and random primers using QuantiTect Reverse Transcription Kit (Qiagen). RT-PCR was performed using the following primers: *Tfap2b*: 5′-CGA CAGCCTCTCGTTGCA-3′ and 5′-TGCTGTCTGTTCAAATAC TCGGA-3′ (WT: 543 bp, *Tfap2b*^{K144}: 543 bp, *Tfap2b*^{K145} long: 541 bp, *Tfap2b*^{K145} short: 424 bp). *Rlp23*: 5′-TTCCGG TCGGAGCTGTGAT-3′ and 5′-CTGCTGGATGTACCTTTTTCCTT (WT: 180 bp). PCR products were purified and subjected to direct sequencing. For *Tfap2b*$^{K145/K145}$, which resulted in PCR products of two different sizes, each product was purified by gel extraction.

Western blot

Western blot was done as previously reported with some modifications (Funato *et al.* 2016). The brain samples were harvested from E18.5 mouse similar to RT-PCR. Tissues were homogenized in ice-cold lysis buffer [20 mM HEPES, pH 7.5, 100 mM NaCl, 10 mM $Na_4P_2O_7$, 1.5% Triton X-100, 15 mM NaF, 1× PhosSTOP (Roche), 5 mM EDTA, 1× protease inhibitor (Roche)], and then centrifuged at 14,000 rpm at 4°. The supernatant were adjusted for 2.5 μg/μl by SDS sample buffer then boiled 95° 5 min and stocked at −30°. The samples were boiled at 95° for 5 min and then separated by SDS-PAGE and transferred on PVDF membrane. Primary antibody was 1/500 rabbit anti TFAP2B (Atlas Antibodies; Cat. No. HPA034683) dissolved in 5% skim milk TBST. Second antibody was 1/5000 rabbit anti HRP (Jackson ImmunoReserarch; Cat. No. 711-035-152) or 1/2000 rabbit anti HRP (Abcam; Cat. No. ab7083) dissolved in 5% skim milk TBST. Clarity Western ECL Substrate (Bio-Rad, Hercules, CA) or Chemi-Lumi One Super (Nacalai Tesque) were used to develop chemiluminescence. The illumination was detected by fusion SOLO5 (Vilber-Lourmat). Then, antibodies were striped by incubating WB Striping Solution Strong (Nacalai Tesque). For detecting β-tubulin as an internal control, rabbit anti β-tubulin (CST; Cat. No. 2128) dissolved in 5% BSA TBST and rabbit anti HRP were used as primary and secondary antibody.

Sleep recording

Electroencephalogram (EEG) and electromyogram (EMG) signals were recorded from freely moving mice at the age of 10–13 weeks following a previous study (Hayashi *et al.* 2015) with some modifications. Briefly, under isoflurane anesthesia (3% induction, 1.5–3% maintenance), mice were placed in a stereotaxic apparatus (David Kopf Instruments). Stainless EEG electrodes were implanted epidurally over the cerebellum and the parietal cortex, and EMG electrodes were embedded into the trapezius muscles bilaterally. At least 4 days after surgery, mice were introduced to the sleep recording apparatus and habituated for at least 5 days. Subsequently, EEG/EMG signals were recorded from the onset of the light phase. EEG/EMG signals were filtered (band pass 0.5–64 Hz or 0.5–250 Hz), collected and digitized at a sampling rate of 128 or 512 Hz using VitalRecorder (Kissei Comtec).

Sleep analysis

EEG/EMG data were divided into 4-s epochs and EEG data were further subjected to fast Fourier transform analysis using SleepSign (Kissei Comtec). The vigilance state in each epoch was manually classified as rapid eye movement sleep (REMS), NREMS, or wake based on absolute delta (0.5–4 Hz) power, theta (6–10 Hz) power to delta power ratio, and the integral of EMG signals. If a single epoch contained multiple states, the state with the highest occupancy was assigned. The EEG power spectrum of each state was calculated and normalized by EEG power at 16–30 Hz averaged across 24 hr (Honda *et al.* 2018). Epochs that either contained multiple stages or presumable large movement-derived artifacts in the EEG data were included in the stage analysis but were excluded from the EEG power spectrum analysis. In addition, only the EEG/EMG data that were collected at 512 Hz were included in the EEG power spectrum analyses.

X-gal staining

Deeply anesthetized mice were killed by injecting lethal doses of anesthetics and underwent transcardial perfusion with 0.1 M PBS followed by 4% paraformaldehyde (w/v) in 0.1 M PBS. The brains were postfixed in the same fixative for 2 hr and subsequently equilibrated in 30% sucrose (w/v) in PBS. The brains were sectioned at 40 μm using a sliding microtome (Yamato Kohki). After washing with PBS, the sections were incubated in 5-bromo-4-chloro-3-indolyl-β-D-galactopyranoside (X-gal) staining solution [0.05% X-gal, 1 mM $MgCl_2$, 3 mM $K_4Fe(CN)_6$, 3 mM $K_3Fe(CN)_6$, and 0.1% Triton X-100 in PBS] at 37°.

Statistics

The experimenter was blinded to the genotype during sleep scoring. All statistical analyses were performed using Prism8 (GraphPad), and statistical significance was set at $P < 0.05$. Where applicable, all statistical tests were two-tailed.

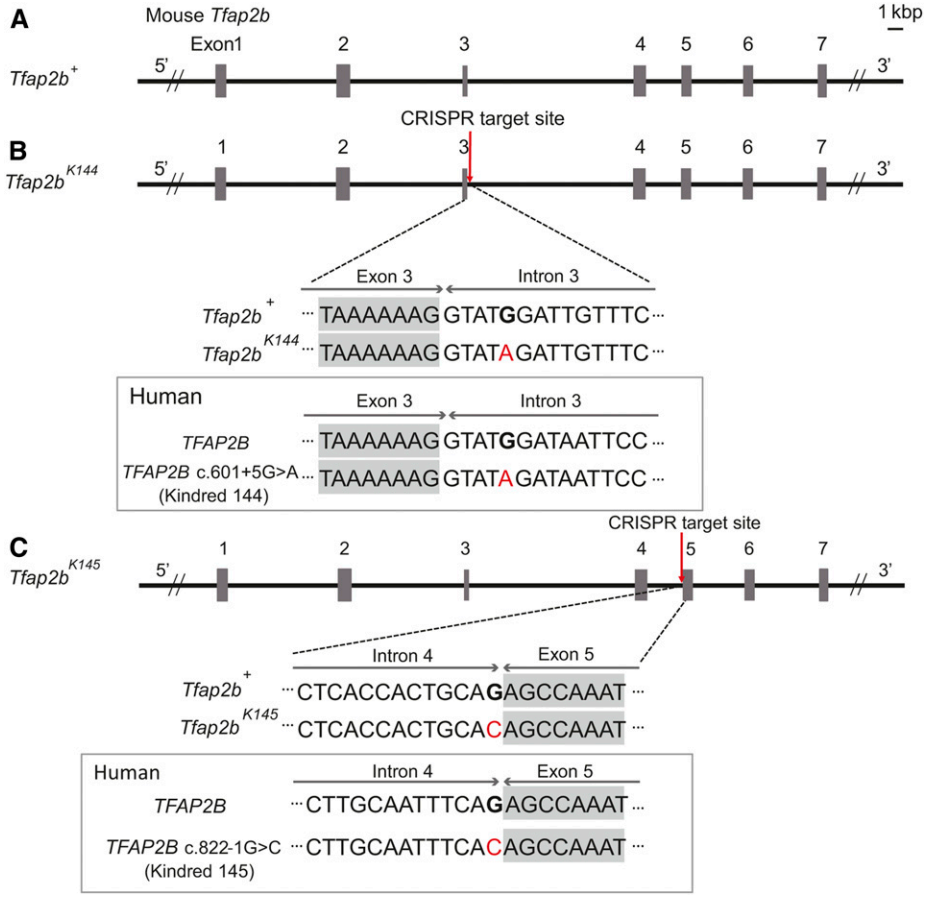

Figure 1 Schematic diagram of the two mutant *Tfap2b* alleles, *Tfap2b*^{K144}, and *Tfap2b*^{K145} generated in this study. (A–C) Genomic structure around *Tfap2b* in WT (A), *Tfap2b*^{K144} (B), and *Tfap2b*^{K145} (C) and comparison of the DNA sequence around the mutation between mouse and human.

Data availability

The authors state that all data necessary for confirming the conclusions presented in the article are represented fully within the article. Further information and requests for reagents should be directed to and will be fulfilled by the corresponding author. Supplemental material available at figshare: https://doi.org/10.25386/genetics.12904568.

Results

Generation of Tfap2b mutant mice that mimic human kindred 144 and 145

We aimed to generate mice that carry mutations in *Tfap2b* (MGI:104672), which mimic the mutations in the human kindreds 144 and 145. In kindred 144, a single base substitution (G to A) at position +5 of the splice donor site of intron three was detected (*TFAP2B* c.601+5G > A), whereas in kindred 145, a single base substitution (G to C) in the splice acceptor site of intron four immediately before exon 5 (*TFAP2B* c.822-1G > C) was detected (Figure 1, A–C) (Mani *et al.* 2005). The genomic DNA sequences around both sites were highly conserved between human and mice (Figure 1, B and C). Using the CRISPR/Cas9 system, we introduced point mutations in mice that each correspond to the mutations in human kindred 144 and 145 (hereafter, *Tfap2b*^{K144} and *Tfap2b*^{K145}, respectively) (Figure 1, B and C). The genomic DNA sequences around the targeted sites in *Tfap2b*^{K144} and *Tfap2b*^{K145} were further confirmed by direct sequencing, and derived cleaved amplified polymorphic sequences (dCAPS) was applied for genotyping of the *Tfap2b* alleles (Supplemental Material, Fig. S1, A–D).

We checked the effects of these mutations on the *Tfap2b* mRNA sequence around exon 3–5, where abnormal splicing due to these mutations are predicted to occur by RT-PCR (Figure 2A) and direct sequencing (Figure S2). Considering that homozygous *Tfap2b* KO mice die shortly after birth (Moser *et al.* 1997), brain samples were collected from the embryos just before birth (embryonic period 18.5; E18.5). As a result, we did not detect any abnormal splicing in *Tfap2b*$^{K144/K144}$ mice (Figure 2A and Figure S2). By contrast, *Tfap2b*$^{K145/K145}$ mice showed very low expression level of Tfap2b mRNA (Figure 2A), and mRNAs of two different lengths were detected (Figure 2B). In the longer mRNA, two nucleotides at the 5′-end of exon 5 was deleted. In the shorter mRNA, exon 5 was completely deleted (Figure S2), likely due to exon skipping. Both variants of Tfap2b mRNA in *Tfap2b*$^{K145/K145}$ mice are predicted to lead to a frame shift (Figure S2).

Next, we checked the effects of these mutations on the TFAP2B protein expression level and molecular weight by

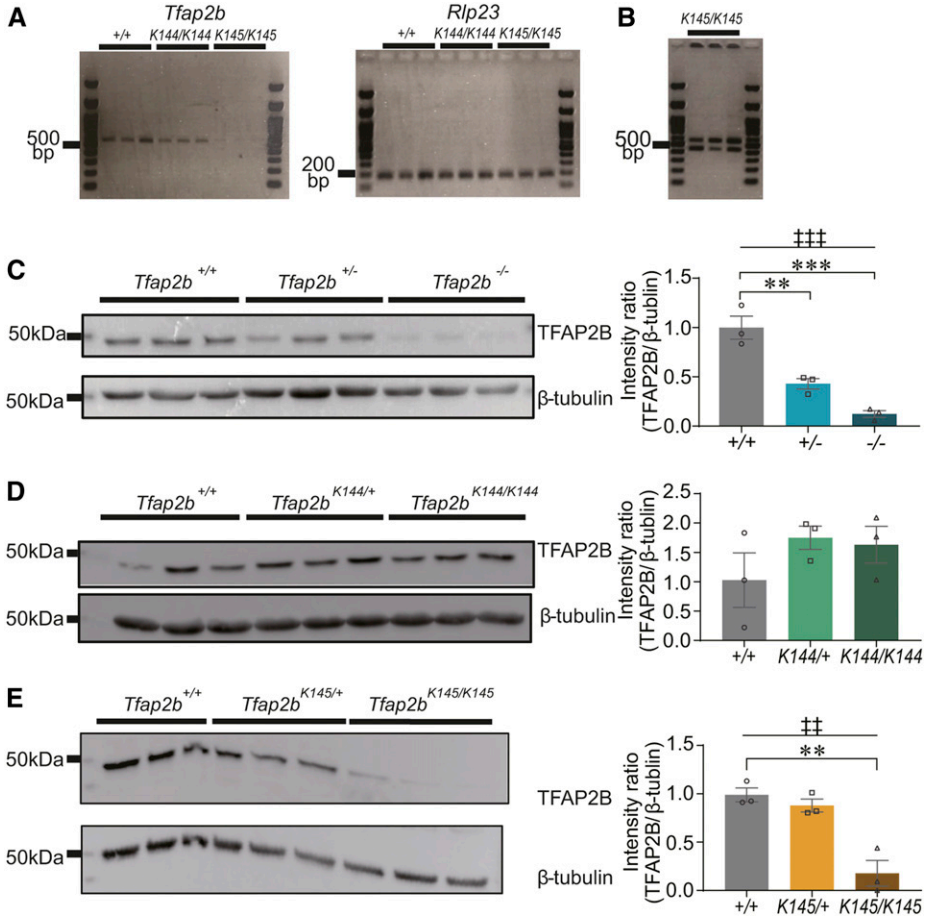

Figure 2 RT-PCR and Western blot analyses of *Tfap2b* mutant mice. (A) Results of RT-PCR using total RNA from whole brain samples of *Tfap2b*$^{+/+}$, *Tfap2b*$^{K144/K144}$, and *Tfap2b*$^{K145/K145}$ mice at E18.5. For RT-PCR of *Tfap2b* mRNA, primers that flank exons 3–5 were used. (B) Increasing amplification cycles of *Tfap2b* RT-PCR in*Tfap2b*$^{K145/K145}$ mice resulted in two products of different size. Each lane represents an individual mouse. $N = 3$ mice. (C–E) Results of Western blot using an anti-TFAP2B antibody applied to whole brain samples from mice at E18.5 harboring *Tfap2b*$^{-}$ (C), *Tfap2b*^{K144} (D), or *Tfap2b*^{K145} (E). Each lane represents an individual mouse. $N = 3$ mice. † indicates significance in one-way ANOVA (‡‡$P < 0.01$, ‡‡‡$P < 0.001$). * indicates significance in *post hoc* Dunnet's test (**$P < 0.01$, ***$P < 0.001$). Data are mean ± SEM.

Western blot using an antibody that recognizes TFAP2B at the region encoded in exon 2. Similar to the above RT-PCR, brain samples were collected from the embryos just before birth (E18.5).We also applied a *Tfap2b* KO allele (*Tfap2b*$^{-}$) (Skarnes *et al.* 2011) to the analysis. The protein expression level was reduced to about half in *Tfap2b*$^{+/-}$ mice and was further reduced in *Tfap2b*$^{-/-}$ mice (Figure 2C). Although exon 1 and exon 2 are intact in *Tfap2b*$^{-}$, no additional bands were detected in samples derived from *Tfap2b*$^{+/-}$ or *Tfap2b*$^{-/-}$ mice, suggesting that the expression level of the truncated TFAP2B protein is very low, if any (Figure S3A). By contrast, we could not detect any effects in *Tfap2b* $^{K144/+}$ and *Tfap2b*$^{K144/K144}$ mice (Figure 2D and Figure S3B). Concerning the *Tfap2b* ^{K145} allele, while no obvious effects were detected in*Tfap2b*$^{K145/+}$ mice, *Tfap2b*$^{K145/K145}$ mice exhibited a significant decrease in the protein expression level that was comparable to *Tfap2b*$^{-/-}$ mice (Figure 2E). Consistently, we never obtained *Tfap2b*$^{K145/K145}$ pups, suggesting that they are lethal. Similar to the other *Tfap2b* alleles, we could not detect any additional bands produced by the *Tfap2b*^{K145} allele (Figure S3C).

Tfap2b$^{+/-}$ female mice show increased wakefulness and decreased NREMS

To test the involvement of *Tfap2b* in sleep regulation, we first compared the sleep architecture between WT and *Tfap2b*$^{+/-}$ mice. The total time spent in wakefulness, NREMS, or REMS was not significantly different between male WT and *Tfap2b*$^{+/-}$ littermates (Figure 3, A and B). The duration and number of episodes of wakefulness and NREMS were not significantly altered either (Figure 4, A and B). The episode number of REMS was slightly increased (Figure 4A).

By contrast, when we compared sleep between female WT and *Tfap2b*$^{+/-}$ littermates, total time spent in wakefulness was increased and NREMS was decreased (Figure 3D). REMS was not significantly different (Figure 3D). When light and dark phases were separately analyzed, we did not detect any interaction between time of the day and the amount of wakefulness or NREMS, but a main effect of genotype was detected, suggesting that the amount of wakefulness and NREMS are affected across the whole day in female *Tfap2b*$^{+/-}$ mice (Figure 3, C and D). Episode analyses revealed that the duration of wakefulness was increased in the dark phase, which might partly account for the increased amount of wakefulness (Figure 4D). The duration and number of episodes of REMS and NREMS were not significantly altered (Figure 4, C and D). When the EEG power spectrum in each stage across 24 hr and the bihourly changes in delta density during NREMS were analyzed, female *Tfap2b*$^{+/-}$ mice showed a trend for decreased delta power during NREMS, although not significant (Figure S4B and Figure S7D). Male *Tfap2b*$^{+/-}$ mice exhibited

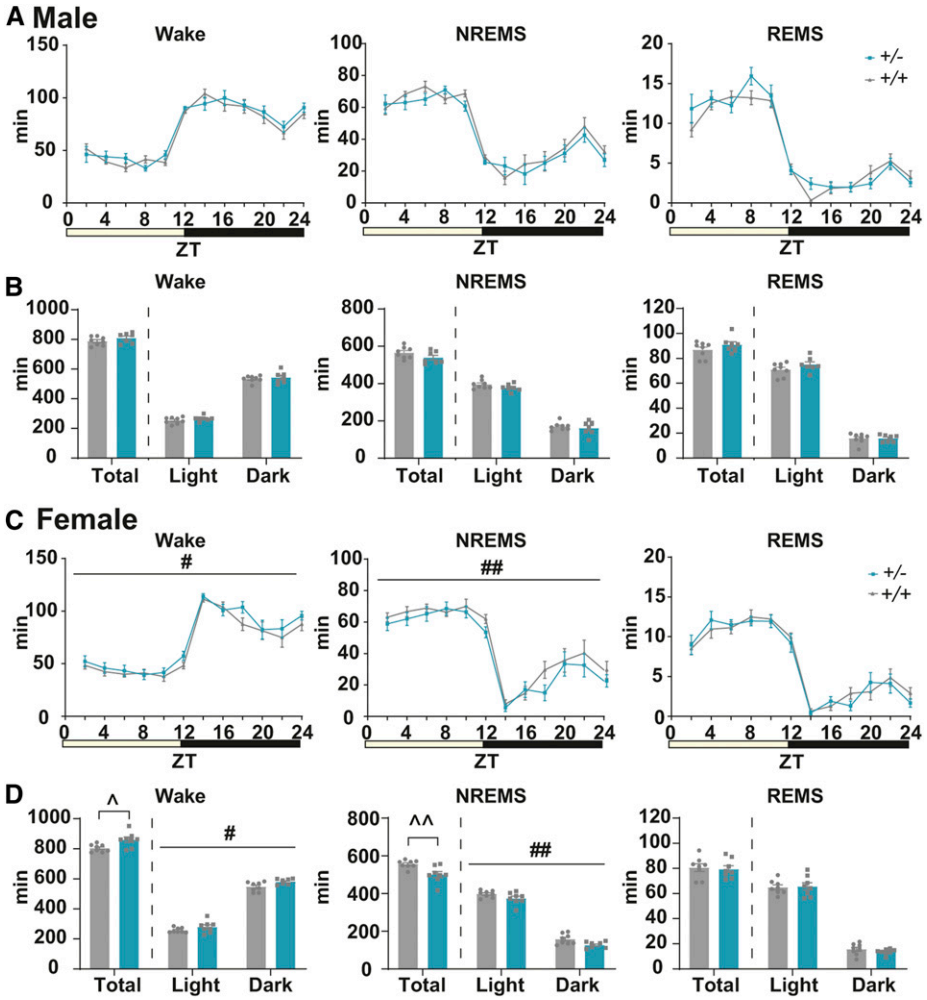

Figure 3 Comparison of the amount of sleep/wake in adult *Tfap2b*$^{+/+}$ and *Tfap2b*$^{+/-}$ mice. (A) Bihourly amount of wakefulness, NREMS, and REMS across 24 hr in male mice. (B) Total amount of wakefulness, NREMS, and REMS during 24 hr, light phase, and dark phase in male mice. $N = 8$ *Tfap2b*$^{+/+}$ mice, $N = 7$ *Tfap2b*$^{+/-}$ mice. (C) Bihourly amount of wakefulness, NREMS, and REMS across 24 hr in female mice. (D) Total amount of wakefulness, NREMS, and REMS during 24 hr, light phase, and dark phase in female mice. $N = 8$ *Tfap2b*$^{+/+}$ mice, $N = 8$ *Tfap2b*$^{+/-}$ mice. $^{\#}$ indicates significant main effect of genotype in two-way repeated-measures ANOVA ($^{\#}P < 0.05$, $^{\#\#}P < 0.01$). ^ indicates significance in the Welch's test ($^{\wedge}P < 0.05$, $^{\wedge\wedge}P < 0.01$). Data are mean ± SEM.

a slight increase in the EEG power 4–4.5 Hz during NREMS, which might have resulted from a slight shift in the peak frequency (Figure S4A).

Tfap2b$^{K145/+}$ *female mice show fragmented NREMS*

Considering that the TFAP2B protein expression level and survival rate were severely affected in *Tfap2b*$^{K145/K145}$ mice, we next examined the sleep architecture of *Tfap2b*$^{K145/+}$ male and female mice. Similar to male *Tfap2b*$^{+/-}$ mice, total time spent in wakefulness, NREMS, or REMS in *Tfap2b*$^{K145/+}$ male mice were not significantly different from WT littermates (Figure 5, A and B). The episode duration and number of each state was also not significantly affected (Figure 6, A and B). During REMS, EEG power in the theta range was slightly reduced (Figure S5A).

Total time spent in wakefulness, NREMS, or REMS was also not significantly affected in female *Tfap2b*$^{K145/+}$ mice (Figure 5, C and D). However, in contrast to female *Tfap2b*$^{+/-}$ mice, the episode number of wakefulness, NREMS, and REMS was increased during the light phase (Figure 6C). In addition, the duration of episodes of NREMS was largely decreased (Figure 6D). These results suggest that the sleep/wake stages are fragmented in the female *Tfap2b*$^{K145/+}$ mice, especially the NREMS in the light phase. The EEG power spectra and NREMS delta density were not significantly affected (Figure S5B and Figure S7E).

Tfap2b$^{K144/+}$ *mice show reduced NREMS in the dark phase*

Next, we compared the sleep architecture between male WT and *Tfap2b*$^{K144/+}$ littermates. *Tfap2b*$^{K144/+}$ mice exhibited a significant decrease in the time spent in NREMS specifically in the dark phase (Figure 7, A and B). This was likely accounted for by a trend for decrease in the number of NREMS episodes (Figure 7C). In addition, during the dark phase, the episode duration of wakefulness was significantly increased, suggesting that each wake episode is more consolidated (Figure 7D). The EEG power spectra and NREMS delta density were not significantly affected (Figure S6 and Figure S7C).

Tfap2b is expressed in the superior colliculus, locus coeruleus, cerebellum, and nucleus of solitary tract

The *Tfap2b*$^{-}$ allele used in this study harbors a *LacZ*-expressing cassette that replaces the original *Tfap2b* gene (Figure

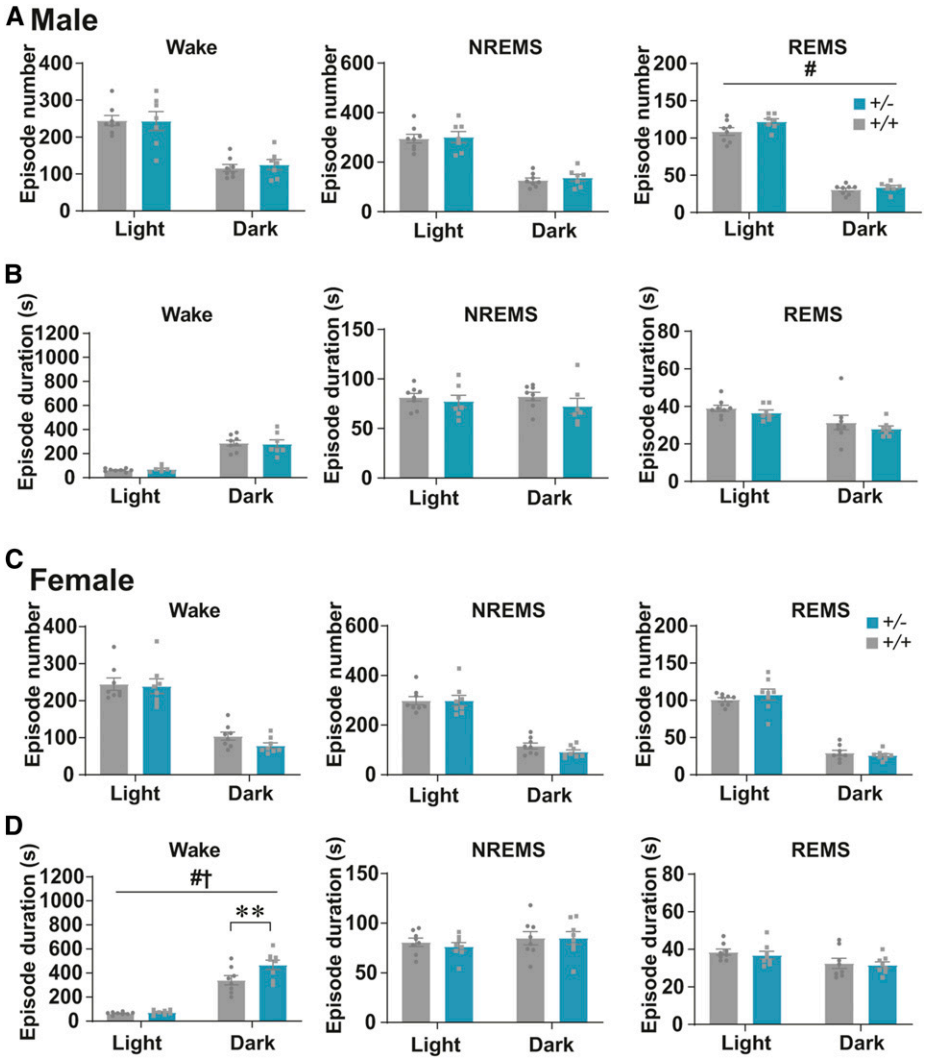

Figure 4 Comparison of the numbers and durations of sleep/wake episodes in adult *Tfap2b*$^{+/+}$ and *Tfap2b*$^{+/-}$ mice. (A, B) Episode numbers (A) and durations (B) of wakefulness, NREMS, and REMS during 24 hr, light phase, and dark phase in male mice. $N = 8$ *Tfap2b*$^{+/+}$ mice, $N = 7$ *Tfap2b*$^{+/-}$ mice. (C, D) Episode numbers (C) and durations (D) of wakefulness, NREMS, and REMS during 24 hr, light phase, and dark phase in female mice. $N = 8$ *Tfap2b*$^{+/+}$ mice, $N = 8$ *Tfap2b*$^{+/-}$ mice. $^{\#}$ and † indicate significant main effect of genotype and significant interaction between genotype and light/dark phase, respectively, in two-way repeated-measures ANOVA ($^{\#,\dagger}P < 0.05$). * indicates significance in *post hoc* Bonferroni multiple comparison test ($^{**}P < 0.01$). Data are mean ± SEM.

8A), thus allowing us to investigate the expression pattern of *Tfap2b* by X-gal staining. X-gal signals were observed in the hypothalamus, midbrain, and hindbrain (Figure 8, B–E). Strong X-gal signals were observed in the superior colliculus (SC; Figure 8C'), cerebellum (Figure 8D'), locus coeruleus (LC; Figure 8D"), and the nucleus of solitary tract (NTS; Figure 8E'), whereas weak signals were detected around the paraventricular hypothalamic nucleus (PVH; Figure 8B'). No signals were detected in the other areas including the olfactory bulb, cerebral cortex, and the preoptic area. TFAP2B locate at cerebellum matured brain, and it is necessary for cerebellum interneuron specification (Zainolabidin *et al.* 2017). Currently, we confirmed the expression in the cerebellum and revealed another site of TFAP2B location in the adult brain.

Discussion

The transcription factor AP-2 has essential roles in developmentally timed sleep or stress-induced sleep in *C. elegans* (Turek *et al.* 2013, 2016; Konietzka *et al.* 2020) and in daily sleep in *D. melanogaster* (Kucherenko *et al.* 2016), suggesting the conserved involvement of this factor in invertebrate sleep. However, the roles of AP-2 in mammalian sleep remained unknown. The current study provides direct evidence showing that the deficiency in TFAP2B affects sleep in mice. Taken together, these studies strongly support that the molecular pathway involving TFAP2B plays a highly conserved role in sleep between mammals and invertebrate animals. Moreover, the current study revealed that mutations in the intron of *Tfap2b* mimicking mutations that were identified in human kindreds with Char syndrome affect sleep in a manner that is largely different from each other or from *Tfap2b* deficiency. Thus, this study provides an important example showing that mutations in a single gene can result in diverse sleep phenotypes, which might explain the diverse nature of sleep-related symptoms in Char syndrome or other familial diseases.

We showed that *Tfap2b*$^{+/-}$ female mice exhibit reduced NREMS and increased wakefulness amounts. This is consistent with the effect of deleting or knocking down the

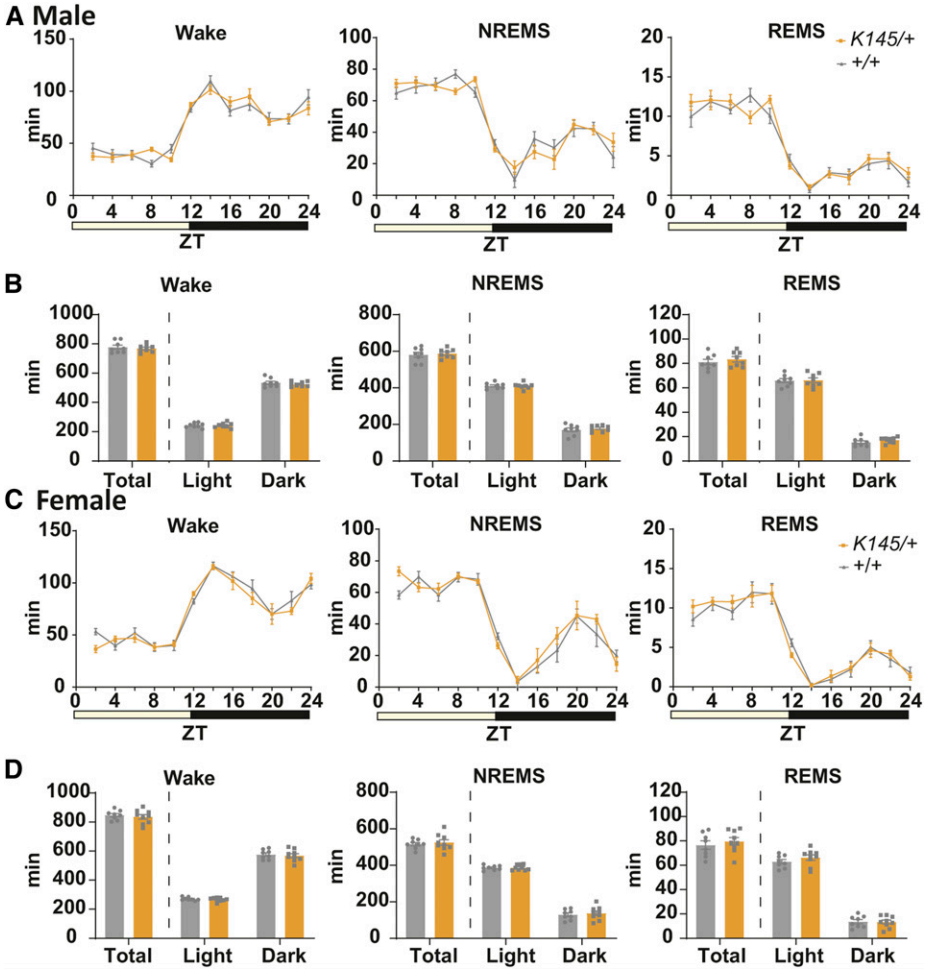

Figure 5 Comparison of the amount of sleep/wake in adult *Tfap2b*$^{+/+}$ and *Tfap2b*$^{K145/+}$ mice. (A) Bihourly amount of wakefulness, NREMS, and REMS across 24 hr in male mice. (B) Total amount of wakefulness, NREMS, and REMS during 24 hr, light phase, and dark phase in male mice. *N* = 8 *Tfap2b*$^{+/+}$ mice, *N* = 8 *Tfap2b*$^{K145/+}$ mice. (C) Bihourly amount of wakefulness, NREMS, and REMS across 24 hr in female mice. (D) Total amount of wakefulness, NREMS, and REMS during 24 hr, light phase, and dark phase in female mice. *N* = 8 *Tfap2b*$^{+/+}$ mice, *N* = 9 *Tfap2b*$^{K145/+}$ mice. Data are mean ± SEM.

orthologs in *C. elegans* or *D. melanogaster* and supports the notion that the molecular mechanism of mammalian NREMS and invertebrate sleep are conserved (Miyazaki *et al.* 2017). We are not sure why male *Tfap2b*$^{+/-}$ mice did not exhibit significantly reduced NREMS, although there was a trend. While female and male mice have similar sleep homeostatic properties, some environmental factors can affect their sleep differently, suggesting that there are some sex differences in the sleep-regulatory mechanisms (Koehl *et al.* 2006). *Tfap2b* deficiency might have affected a sleep regulatory pathway that is more vulnerable in females.

In contrast to *Tfap2b*$^{+/-}$ mice, *Tfap2b*$^{K145/+}$ female mice did not exhibit reduced NREMS amount but instead exhibited fragmented NREMS. The TFAP2B protein expression level was decreased to a similar extent in *Tfap2b*$^{-/-}$ and *Tfap2b*$^{K145/K145}$ mice. *Tfap2b*^{K145} harbors a single base substitution within the highly conserved splice acceptor sequence (AG) immediately before exon 5. Thus, *Tfap2b*^{K145} was predicted to lead to the skipping of exon 5 (Mani *et al.* 2005). Indeed, in the *Tfap2b*$^{K145/K145}$ mice, we detected a shortened *Tfap2b* mRNA in which exon 5 was missing. In addition, we also detected a *Tfap2b* mRNA in which only two nucleotides at the 5′-end of exon 5 was deleted. In both cases, the variation in the mRNA sequence leads to a frame shift. The mRNA expression level was also largely decreased in the *Tfap2b*$^{K145/K145}$ mice, likely due to nonsense mediated decay. While this can explain why the TFAP2B protein expression level was largely decreased in *Tfap2b*$^{K145/K145}$ mice, it remains unknown why *Tfap2b*$^{K145/+}$ mice and *Tfap2b*$^{+/-}$ mice exhibit totally different sleep phenotypes. Unlike *Tfap2b*$^{+/-}$ mice, *Tfap2b*$^{K145/+}$ mice did not exhibit an obvious reduction in TFAP2B protein, which might be a result of enhanced transcription of the WT allele by mechanisms of transcriptional adaptation (El-Brolosy *et al.* 2019). In addition to nonsense mediated decay, *Tfap2b*^{K145} might cause some effect on the protein that is different from *Tfap2b*$^{-}$. For example, a small proportion of the mRNA derived from *Tfap2b*^{K145} might be translated, resulting in the expression of an abnormal protein that interferes with the function of the WT TFAP2B protein.

The sleep phenotype of *Tfap2b*$^{K144/+}$ mice also differed from the other *Tfap2b* mutants. Male *Tfap2b*$^{K144/+}$ mice showed reduced NREMS during the dark phase. *Tfap2b*^{K144} harbors a single base substitution within the putative splice donor sequence immediately after exon 3. In human cells, this mutation leads to the skipping of exon 3 (Mani *et al.* 2005). If exon 3 is skipped in *Tfap2b*^{K144}, it will cause a frame shift and premature termination codon that would lead to

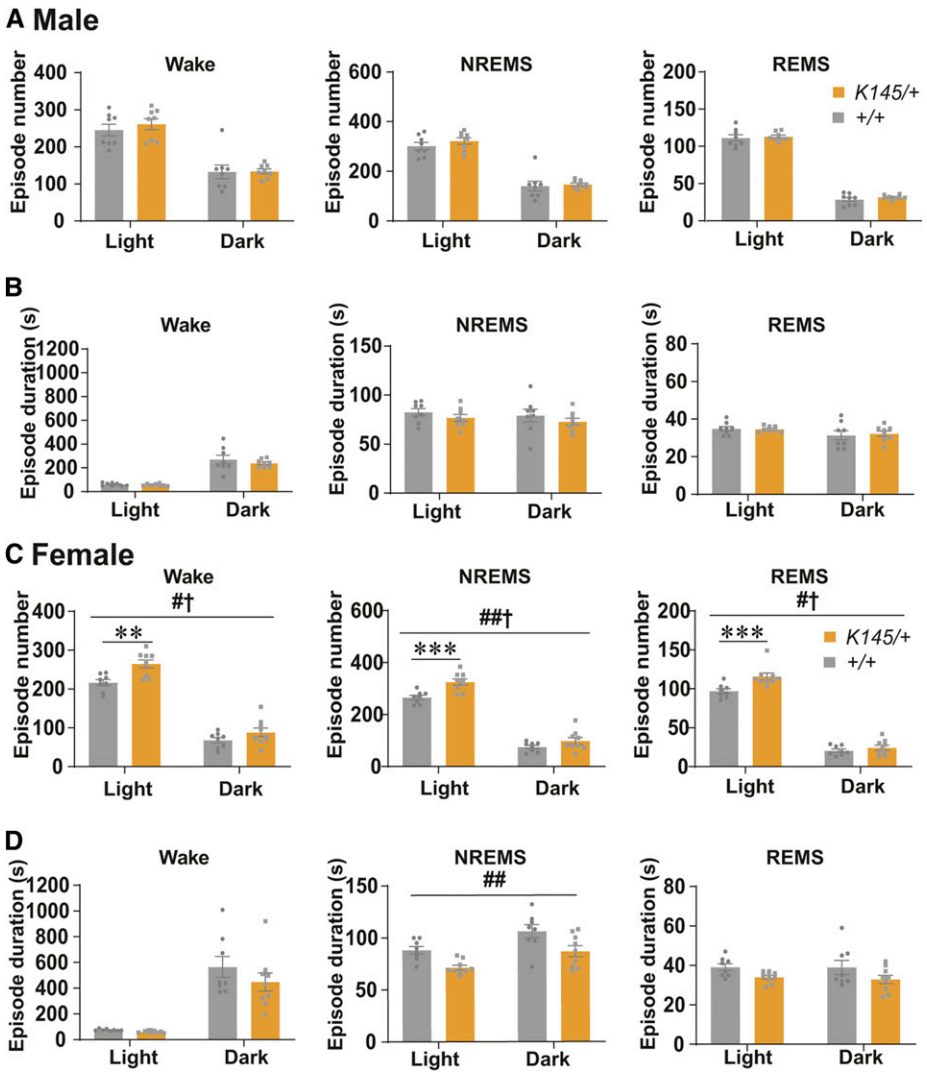

Figure 6 Comparison of the sleep episode number and duration in adult *Tfap2b*$^{+/+}$ and *Tfap2b*$^{K145/+}$ mice. (A, B) Episode numbers (A) and durations (B) of wakefulness, NREMS, and REMS during 24 hr, light phase, and dark phase in male mice. $N = 8$ *Tfap2b*$^{+/+}$ mice, $N = 8$ *Tfap2b*$^{K145/+}$ mice. (C and D) Episode numbers (C) and durations (D) of wakefulness, NREMS, and REMS during 24 hr, light phase, and dark phase in female mice. $N = 8$ *Tfap2b*$^{+/+}$ mice, $N = 9$ *Tfap2b*$^{K145/+}$ mice. $^{\#}$ and † indicate significant main effect of genotype and significant interaction between genotype and light/dark phase, respectively, in two-way repeated-measures ANOVA ($^{\#,\dagger}P < 0.05$, $^{\#\#}P < 0.01$). * indicates significance in *post hoc* Bonferroni multiple comparison test ($^{**}P < 0.01$, $^{***}P < 0.001$). Data are mean ± SEM.

either the production of a truncated protein or nonsense mediated decay of the mRNA. However, in case of the *Tfap2b*^{K144} allele, we did not detect any effects on the *Tfap2b* mRNA expression level nor sequence. Moreover, we did not detect any effects on the TFAP2B protein expression level nor the molecular weight even in homozygotes. In addition, unlike *Tfap2b*$^{K145/K145}$ mice, *Tfap2b*$^{K144/K144}$ mice were viable. Thus, further analyses are required to reveal how the mutation affects the properties of TFAP2B. Another possibility might be that, considering that *cis*-elements of transcriptional regulation can exist in introns, *Tfap2b*^{K144} might affect the expression pattern of *Tfap2b*.

In the adult brain, *Tfap2b* expression was detected in the SC, LC, cerebellum and NTS. Within these areas, the SC is implicated in the acute induction of sleep triggered by light stimulation during the dark phase, although its dysfunction does not affect baseline sleep (Miller *et al.* 1998). By contrast, LC contains wake promoting neurons (Aston-Jones and Bloom 1981), and global or local deletion of dopamine β-hydroxylase, which is essential for the synthesis of noradrenalin in LC, results in reduced wakefulness and increased NREMS (Carter *et al.* 2010; Yamaguchi *et al.* 2018). Thus, although deletion of *Tfap2b* leads to reduced expression of dopamine β-hydroxylase in the LC (Seok *et al.* 2008), we are not sure whether it can explain the observed sleep phenotypes in this study. *Tfap2b* is more widely expressed in the embryonic brain (Thompson *et al.* 2014), and it might play a crucially role in the differentiation of sleep-promoting neurons. The mechanisms of sleep regulation by AP-2 transcription factors are best studied in *C. elegans*. In *C. elegans*, the GABAergic neuron RIS plays a crucial role in the induction of sleep (Turek *et al.* 2013). The *C. elegans* ortholog APTF-1 is selectively expressed in RIS, and APTF-1 exerts its sleep-promoting effect by promoting the transcription of the neuropeptide FLP-11 in RIS (Turek *et al.* 2016). Thus, TFAP2B might contribute to mouse sleep regulation by promoting the transcription or syntheses of neuropeptides or other neuromodulators within sleep-promoting neurons.

While we successfully showed that mutations in *Tfap2b* can differently affect sleep, the effects of *Tfap2b*^{K144} and

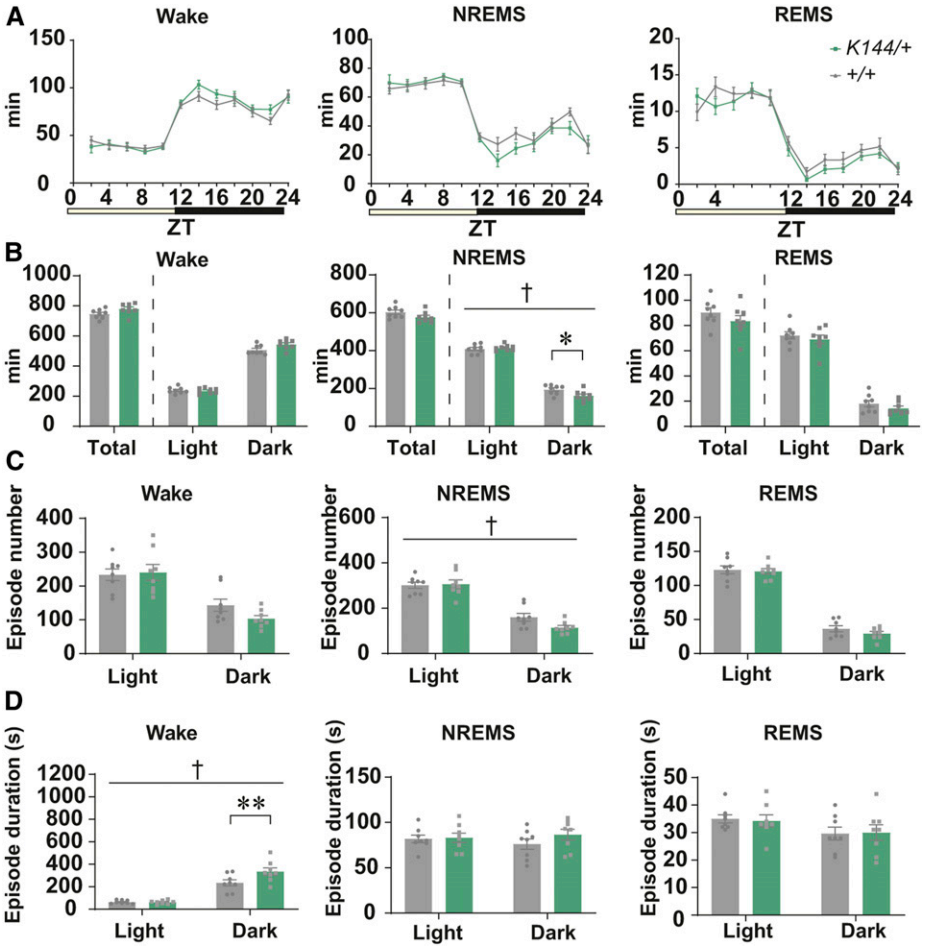

Figure 7 Comparison of the sleep architecture in adult *Tfap2b*$^{+/+}$ and *Tfap2b*$^{K144/+}$ mice. (A) Bihourly amount of wakefulness, NREMS, and REMS across 24 hr in male mice. (B) Total amount of wakefulness, NREMS, and REMS during 24 hr, light phase, and dark phase in male mice. (C, D) Episode durations (C) and numbers (D) of wakefulness, NREMS, REMS during 24 hr, light phase, and dark phase in male mice. $N = 8$ *Tfap2b*$^{+/+}$ mice, $N = 8$ *Tfap2b*$^{K144/+}$ mice. † indicates significant interaction between genotype and Zeitgeber time (ZT) or light/dark phase in two-way repeated-measures ANOVA ($^{\dagger}P < 0.05$). * indicates significance in *post hoc* Bonferroni multiple comparison test ($^{*}P < 0.05$, $^{**}P < 0.01$). Data are mean ± SEM.

Tfap2b^{K145} on mouse sleep did not match the sleep-related symptoms that were self-reported by the human kindreds 144 and 145. In humans, kindred 144 self-reported parasomnia. However, although we monitored mice behaviors by video recording together with EEG/EMG recording, we never observed any abnormal movements during sleep in any of the *Tfap2b* mutants. In addition, kindred 145 self-reported short sleep, whereas *Tfap2b*$^{K145/+}$ mice exhibited fragmented

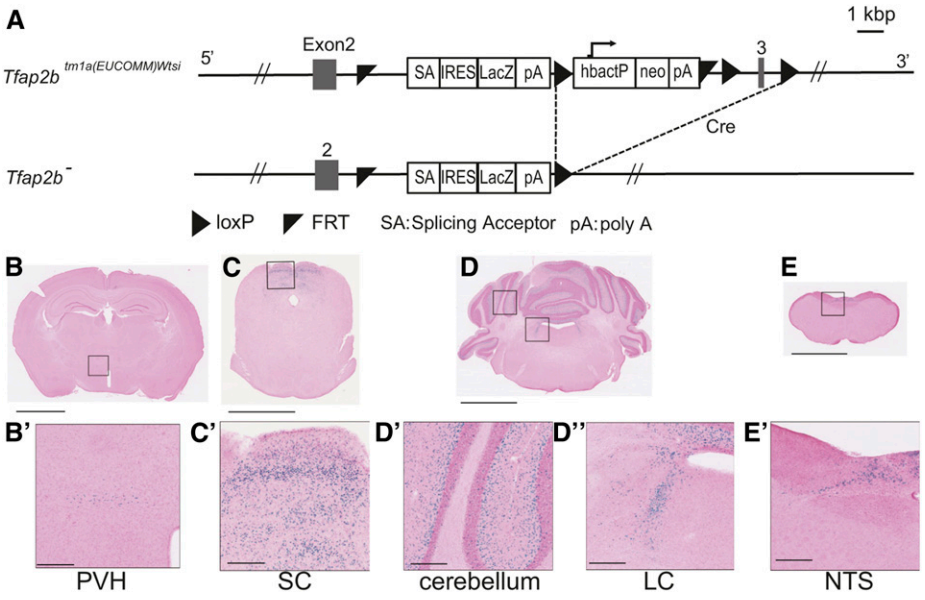

Figure 8 Expression analyses of *Tfap2b* in the adult brain by X-gal staining of *Tfap2b*$^{+/-}$ mice. (A) Schematic diagram of the *Tfap2b*$^{-}$ allele used in this study. (B–E) Images of areas where LacZ-derived signals were detected. PVH, paraventricular hypothalamic nucleus (B'); SC, superior colliculus (C'); LC, locus coeruleus (D''); NTS, solitary tract nucleus (E'). Bars: B–E, 2.5 mm; B'–E', 250 μm. Representative images from a replicate of three mice are shown.

sleep. There is a possibility that the effects of the mutations in *Tfap2b* might differ depending on the species or other genetic backgrounds. In addition, the human studies on kindreds 144 and 145 did not conduct polysomnography recording, and thus the self-reports on sleep might not be accurate.

In summary, by generating *Tfap2b*^{K144} and *Tfap2b*^{K145} mutant mice and comparing their sleep with *Tfap2b*$^{+/-}$ mice, we show that *Tfap2b* is involved in the regulation of sleep in mice and that different mutations within *Tfap2b* have diverse effects on sleep. This study further supports the important and complicated roles of AP-2 transcription factors in sleep regulation.

Acknowledgments

We thank Risa Yamazaki for technical advice. This study was supported by the Japan Society for the Promtion of Science (JSPS) KAKENHI grant number JP20H03353, Japan Agency for Medical Research and Development (AMED) under grant numbers JP19dm0107138 and JP19gm1110008 (to Y.H.), Japan Science and Technology Agency (JST) under grant number JPMJCR1655 and the Ministry of Education, Culture, Sports, Science and Technology (MEXT)/JSPS World Premier International Research Center (WPI) program (to M.Y. and Y.H.).

Literature Cited

Aston-Jones, G., and F. E. Bloom, 1981 Activity of norepinephrine-containing locus coeruleus neurons in behaving rats anticipates fluctuations in the sleep-waking cycle. J. Neurosci. 1: 876–886. https://doi.org/10.1523/JNEUROSCI.01-08-00876.1981

Carter, M. E., O. Yizhar, S. Chikahisa, H. Nguyen, A. Adamantidis *et al.*, 2010 Tuning arousal with optogenetic modulation of locus coeruleus neurons. Nat. Neurosci. 13: 1526–1535. https://doi.org/10.1038/nn.2682

Davidson, H. R., 1993 A large family with patent ductus arteriosus and unusual face. J. Med. Genet. 30: 503–505. https://doi.org/10.1136/jmg.30.6.503

Eckert, D., S. Buhl, S. Weber, R. Jäger, and H. Schorle, 2005 The AP-2 family of transcription factors. Genome Biol. 6: 246. https://doi.org/10.1186/gb-2005-6-13-246

El-Brolosy, M. A., Z. Kontarakis, A. Rossi, C. Kuenne, S. Günther *et al.*, 2019 Genetic compensation triggered by mutant mRNA degradation. Nature 568: 193–197. https://doi.org/10.1038/s41586-019-1064-z

Funato, H., C. Miyoshi, T. Fujiyama, T. Kanda, M. Sato *et al.*, 2016 Forward-genetics analysis of sleep in randomly mutagenized mice. Nature 539: 378–383. https://doi.org/10.1038/nature20142

Hayashi, Y., M. Kashiwagi, K. Yasuda, R. Ando, M. Kanuka *et al.*, 2015 Cells of a common developmental origin regulate REM/non-REM sleep and wakefulness in mice. Science 350: 957–961. https://doi.org/10.1126/science.aad1023

Honda, T., T. Fujiyama, C. Miyoshi, A. Ikkyu, N. Hotta-Hirashima *et al.*, 2018 A single phosphorylation site of SIK3 regulates daily sleep amounts and sleep need in mice. Proc. Natl. Acad. Sci. USA 115: 10458–10463. https://doi.org/10.1073/pnas.1810823115

Hong, S. J., T. Lardaro, S. O. Myung, Y. Huh, Y. Ding *et al.*, 2008 Regulation of the noradrenaline neurotransmitter phenotype by the transcription factor AP-2β. J. Biol. Chem. 283: 16860–16867. https://doi.org/10.1074/jbc.M709106200

Jin, K., H. Jiang, D. Xiao, M. Zou, J. Zhu *et al.*, 2015 Tfap2a and 2b act downstream of Ptf1a to promote amacrine cell differentiation during retinogenesis. Mol. Brain 8: 28. https://doi.org/10.1186/s13041-015-0118-x

Koehl, M., S. Battle, and P. Meerlo, 2006 Sex differences in sleep: the response to sleep deprivation and restraint stress in mice. Sleep 29: 1224–1231. https://doi.org/10.1093/sleep/29.9.1224

Konietzka, J., M. Fritz, S. Spiri, R. McWhirter, A. Leha *et al.*, 2020 Epidermal growth factor signaling promotes sleep through a combined series and parallel neural circuit. Curr. Biol. 30: 1–16.e13. https://doi.org/10.1016/j.cub.2019.10.048

Kucherenko, M. M., V. Ilangovan, B. Herzig, H. R. Shcherbata, and H. Bringmann, 2016 TfAP-2 is required for night sleep in Drosophila. BMC Neurosci. 17: 72. https://doi.org/10.1186/s12868-016-0306-3

Mani, A., J. Radhakrishnan, A. Farhi, K. S. Carew, C. A. Warnes *et al.*, 2005 Syndromic patent ductus arteriosus: evidence for haploinsufficient TFAP2B mutations and identification of a linked sleep disorder. Proc. Natl. Acad. Sci. USA 102: 2975–2979. https://doi.org/10.1073/pnas.0409852102

Miller, A. M., W. H. Obermeyer, M. Behan, and R. M. Benca, 1998 The superior colliculus-pretectum mediates the direct effects of light on sleep. Proc. Natl. Acad. Sci. USA 95: 8957–8962. https://doi.org/10.1073/pnas.95.15.8957

Miyazaki, S., C. Y. Liu, and Y. Hayashi, 2017 Sleep in vertebrate and invertebrate animals, and insights into the function and evolution of sleep. Neurosci. Res. 118: 3–12. https://doi.org/10.1016/j.neures.2017.04.017

Moser, M., A. Pscherer, C. Roth, J. Becker, G. Mücher *et al.*, 1997 Enhanced apoptotic cell death of renal epithelial cells in mice lacking transcription factor AP-2β. Genes Dev. 11: 1938–1948. https://doi.org/10.1101/gad.11.15.1938

Moser, M., S. Dahmen, R. Kluge, H. Gröne, J. Dahmen *et al.*, 2003 Terminal renal failure in mice lacking transcription factor AP-2β. Lab. Invest. 83: 571–578. https://doi.org/10.1097/01.LAB.0000064703.92382.50

Niwa, H., K. Araki, S. Kimura, S. I. Taniguchi, S. Wakasugi *et al.*, 1993 An efficient gene-trap method using poly a trap vectors and characterization of gene-trap events. J. Biochem. 113: 343–349. https://doi.org/10.1093/oxfordjournals.jbchem.a124049

Satoda, M., F. Zhao, G. A. Diaz, J. Burn, J. Goodship *et al.*, 2000 Mutations in TFAP2B cause Char syndrome, a familial form of patent ductus arteriosus. Nat. Genet. 25: 42–46. https://doi.org/10.1038/75578

Sato, Y., H. Tsukaguchi, H. Morita, K. Higasa, M. T. N. Tran *et al.*, 2018 A mutation in transcription factor MAFB causes focal segmental glomerulosclerosis with duane retraction syndrome. Kidney Int. 94: 396–407. https://doi.org/10.1016/j.kint.2018.02.025

Seki, R., K. Kitajima, H. Matsubara, T. Suzuki, D. Saito *et al.*, 2015 AP-2β is a transcriptional regulator for determination of digit length in tetrapods. Dev. Biol. 407: 75–89. https://doi.org/10.1016/j.ydbio.2015.08.006

Shi, G., D. Wu, L. J. Ptáček, and Y. H. Fu, 2017 Human genetics and sleep behavior. Curr. Opin. Neurobiol. 44: 43–49. https://doi.org/10.1016/j.conb.2017.02.015

Skarnes, W. C., B. Rosen, A. P. West, M. Koutsourakis, W. Bushell *et al.*, 2011 A conditional knockout resource for the genome-wide study of mouse gene function. Nature 474: 337–342. https://doi.org/10.1038/nature10163

Thompson, C. L., L. Ng, V. Menon, S. Martinez, C. K. Lee *et al.*, 2014 A high-resolution spatiotemporal atlas of gene expression of the developing mouse brain. Neuron 83: 309–323. https://doi.org/10.1016/j.neuron.2014.05.033

Turek, M., I. Lewandrowski, and H. Bringmann, 2013 An AP2 transcription factor is required for a sleep-active neuron to induce sleep-like quiescence in C. elegans. Curr. Biol. 23: 2215–2223. https://doi.org/10.1016/j.cub.2013.09.028

Turek, M., J. Besseling, J. P. Spies, S. König, and H. Bringmann, 2016 Sleep-active neuron specification and sleep induction require FLP-11 neuropeptides to systemically induce sleep. eLife 5: e12499. https://doi.org/10.7554/eLife.12499

Yamaguchi, H., F. W. Hopf, S. Bin Li, and L. de Lecea, 2018 In vivo cell type-specific CRISPR knockdown of dopamine beta hydroxylase reduces locus coeruleus evoked wakefulness. Nat. Commun. 9: 5211. https://doi.org/10.1038/s41467-018-07566-3

Zainolabidin, N., S. P. Kamath, A. R. Thanawalla, and A. I. Chen, 2017 Distinct activities of tfap2a and tfap2b in the specification of GABaergic interneurons in the developing cerebellum. Front. Mol. Neurosci. 10: 281. https://doi.org/10.3389/fnmol.2017.00281

Communicating editor: J. Schimenti